Available online at www.sciencedirect.com
SCIENCE DIRECT®
International Journal of Mass Spectrometry 233 (2004) 199–205
International Journal of Mass Spectrometry
www.elsevier.com/locate/ijms

Low energy electron attachment by bromoalkanes

Wiesława Barszczewska, Janina Kopyra, Jolanta Wnorowska, Iwona Szamrej*

Chemistry Department, University of Podlasie, Siedlce 08-110, Poland

Received 9 October 2003; accepted 21 December 2003

Abstract

Thermal electron attachment processes in the mixtures of $CH_3CH_2CH_2Br$, $CH_3CHBrCH_3$, CH_2BrCH_2Br, CH_2FCH_2Br and CF_3CH_2Br with carbon dioxide have been investigated using an electron swarm method. It has been found that all the investigated compounds attach electrons only in a two-body process. Corresponding rate constants have been determined to be equal to 1.1×10^{-11}, 1.4×10^{-12}, 1.8×10^{-8}, 5×10^{-11} and 1.4×10^{-9} cm^3 $molecule^{-1}$ s^{-1}, respectively. The dependence of the electron capture rate constants on electronic polarizability of the accepting center of the molecule has been demonstrated. The average rate constant for CH_3Br, CH_3CH_2Br and $CH_3CH_2CH_2Br$ equal to $(6 \pm 2) \times 10^{-12}$ cm^3 $molecule^{-1}$ s^{-1} is recommended.

Keywords: Electron attachment; Negative ions; Electron swarm; Halocarbons

1. Introduction

Low-energy electron attachment studies provide fundamental information on electron–molecule interaction, which is of practical importance for many applications such as gaseous electronics, gas laser technology, aerospace communications and atmospheric chemistry.

Thermal energy electrons can be effectively captured in the gas phase by many molecules in a two-body process with formation of an excited negative ion (reaction 1)

$$e^- + AB \rightarrow AB^{*-} \quad (1)$$

which further undergoes reactions (2)–(5):

$$AB^{*-} \rightarrow AB + e^- \quad \text{(autodetachment)} \quad (2)$$

$$AB^{*-} \rightarrow AB^- + h\nu \quad \text{(radiative stabilization)} \quad (3)$$

$$AB^{*-} \rightarrow AB^- \quad \text{(internal stabilization)} \quad (4)$$

$$AB^{*-} \rightarrow A^- + B \text{ (or } A + B^-) \quad \text{(dissociation)} \quad (5)$$

Stabilization can also be achieved in a collision with a third body (reaction 6).

$$AB^{*-} + M \rightarrow AB^- + M \quad (6)$$

The second order rate constants for the thermal electron capture have been determined for a long time in many laboratories with a wide spectrum of different experimental techniques. However, not too many compounds have been investigated. Moreover, in most cases a large scattering of the results from different laboratories is observed. This could be caused either by not achieving the truly thermal distribution of electron energy or neglecting a contribution from higher order electron attachment processes.

Two-body rate constants obtained in different laboratories differ sometimes by more than an order of magnitude. So there is a need for seeking a method, which helps to verify these values as well as to find the connection between the structure of the molecule and its ability to capture an electron.

There are also some data on the higher than second order electron attachment processes, both collisionaly stabilized attachment and attachment by van der Waals (vdW) complexes. The last process can be described exactly the same way as the attachment by individual molecule (reactions 1–5), but the medium, which accepts electron, is a vdW dimer consisting of two of the same or different molecules.

We have started the systematic investigation of the electron capture processes by haloalkanes to get a clearer picture of how the effectiveness and the mechanism of the electron attachment depends on the structure of the attaching molecule. This is probably the largest and most thoroughly investigated homologous group of compounds. The electron

* Corresponding author. Tel.: +48-25-6431032.
E-mail address: iwona@ap.siedlce.pl (I. Szamrej).

1387-3806/$ – see front matter © 2004 Elsevier B.V. All rights reserved.
doi:10.1016/j.ijms.2003.12.018

capture by halogenated hydrocarbons is interesting also from the practical point of view. They play important and very harmful role in the atmosphere, not only destroying the ozone layer but also acting as the greenhouse agents. To diminish their negative influence on the environment it is necessary to find methods, which destroy halocarbons existing in the atmosphere. The knowledge of electron attachment processes is of primary importance also for this purpose.

In our previous papers we have presented results on the thermal electron capture by halomethanes [1–3]. In almost all the cases we have found out that in the electron capture both individual molecules and vdW dimers are involved. The only exception was shown for methyl bromide where only the two-body process has been found. The situation differs entirely for haloethanes and halopropanes, where only the two-body processes have been observed. Continuing these systematic investigations we have now started to measure rate constants for bromopropanes. In this paper we present the results we have got for halocarbons containing bromine.

2. Experimental procedure

The experimental set-up used for the investigations is presented in Fig. 1. It consists of an ionization chamber (1) with two parallel electrodes (a) and (b), a Canberra-Packard preamplifier model 2006 (2), a fast (50 ns) oscilloscope with digital memory (3) connected with a computer and a computer-controlled Canberra-Packard dual 0–5 kV HV power supply model 3125 [4].

The electron swarm is produced by an α-particle in the plane of an α-particle source (c). The electron swarm moves to the collecting electrode (a) traversing a distance d (ca. 2 cm) under the influence of a uniform electric field, E, applied between the electrodes. To minimize the influence of the α-source ring it is kept at a zero potential. The drift velocity, W, is a function of the density-reduced electric field, E/N, where N is the total density of the gas in the chamber. In the case of thermal electrons $W = \mu_N \times E/N$, where μ_N denotes the density-normalized electron mobility.

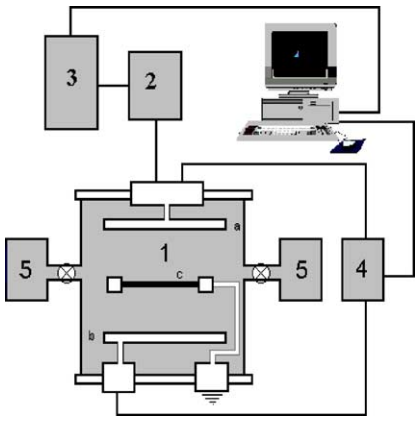

Fig. 1. The experimental set-up used in this investigation (for details see text).

The output pulse from the preamplifier is registered in the digital memory of the oscilloscope. The data are further transferred to the computer memory. The preamplifier converts the input signal from the collecting electrode into an output voltage pulse (whose amplitude is proportional to that of the input signal) with the rise time less than 35 ns. The exponential decay time, t_1, of the pulse is equal to 46 μs (both the values were checked with a step function generator). The electrons traverse the distance d at a time t_0 in the range of 1–50 μs, depending on applied E/N. Thus, we can put that preamplifier follows "immediately" the changes in the electrode potential and discharges both during the pulse and afterwards. It means that the total response function of the preamplifier is that of the decay. To get the shape of the pulse registered by the oscilloscope we have followed the considerations presented in our previous paper [4].

The experiment was performed in such a way that each haloalkane–carbon dioxide mixture was first introduced into the chamber at the highest applied total pressure (ca. 1000 Torr). Always 700 pulses were registered for a given E/N and averaged as described above. The procedure was repeated usually for five E/N values in the rather wide range (6×10^{-18} to 3×10^{-17} V cm^2 molecule^{-1}), where electrons in carbon dioxide are in thermal equilibrium with gas molecules. Next, the mixture was pumped-out to a lower pressure and the measurement procedure was repeated (for ca. 15 consecutive pressures in the range 300–1000 Torr). The whole experiment was carried out for a few different initial concentrations of haloalkane in carbon dioxide.

The one of most important factors in measuring the electron capture rate constants is a purity of an electron acceptor, especially for those with a rather low rate constant value as in the case of monobromo-substituted alkanes because further substitution causes increase in the rate constant by several orders of magnitude and only minute impurities of that kind can cause drastic change in the measured rate constants. The purity of haloalkanes stated by manufacturers is usually no better than 99% and the nature of impurities is not shown. The usual freeze–pump–thaw technique consists of degassing at liquid nitrogen temperature (cf. ref. [19]). This however does not remove those most dangerous impurities, as they are less volatile. To remove these impurities in each case we prepared a bath with temperature at which the investigated compound has a vapor pressure of a few Torr. It was achieved by choosing a compound with proper melting point and freezing it with liquid nitrogen. For methyl bromide, e.g., it is acetone with mp −94.6 °C at which CH_3Br vapor pressure is ca. 2 Torr and that for CH_2Br_2 well below 10^{-3} Torr.

Another important precaution from this point of view is not to measure the rate constants for monosubstituted alkanes immediately after using multi-substituted ones without special care as the last except of having high rate constant also absorb strongly. This was also taken into account in our experiment.

All measurements were carried out at room temperature (293 ± 5 K).

3. Results and discussion

We have measured kinetics of thermal electron attachment processes by $CH_3CH_2CH_2Br$, $CH_3CHBrCH_3$, CH_2BrCH_2Br, CH_2FCH_2Br and CF_3CH_2Br diluted with carbon dioxide. Examples of results for $CH_3CH_2CH_2Br$ and $CH_3CHBrCH_3$ in terms of the rate of electron disappearance from the swarm versus halocarbon concentration for different concentrations of CO_2 as a diluting gas are shown in Fig. 2. The very good straight lines as well as zero intercepts show that in all presented cases only the two-body electron attachment processes take place. All measured rate constants together with our previous results and the available literature data on bromo- and bromofluoro-derivatives of methane, ethane and propane are presented in Table 1. It can be seen that the rate constants obtained in different laboratories vary strongly, sometimes by more than order of magnitude. So it is often difficult to judge the validity of new results by comparison with the literature data. However, for some cases there are repeatable results, which can be safely averaged, and serve as guiding ones for further consideration. They are also shown in Table 1 together with those calculated by Christophorou [26]. A need to find the link between the value of the rate constant and molecular parameters is obvious both from theoretical and practical point of view.

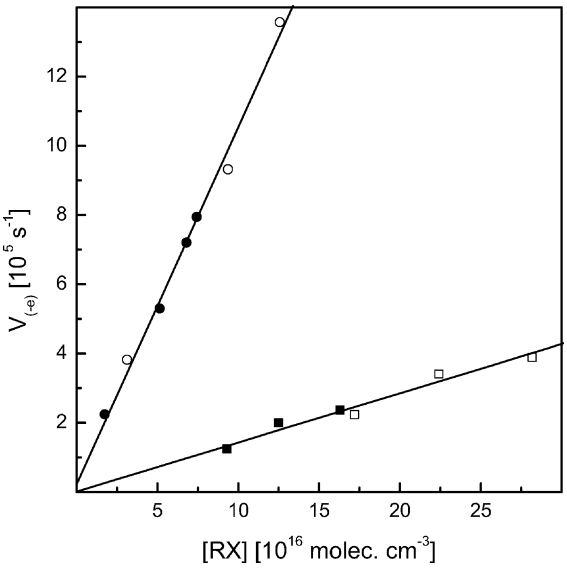

Fig. 2. The rate of electron disappearance from the swarm as a function of halocarbon concentration: (○) $CH_3CH_2CH_2Br$, (□) $CH_3CHBrCH_3$ at 0.9×10^{18} molecule cm^{-3} of CO_2 (■, 3×10^{18} molecule cm^{-3} of CO_2).

For this purpose one can consider such characteristics as a dipole moment of the molecule or the bond, μ, an electronic polarizability, α, total molecular polarizability $\alpha + \mu^2/3kT$,

Table 1
The rate constants for electron capture by bromine containing halocarbons together with corresponding values of α_{center}

Compound	α_{center} ($\times 10^{-24}$ cm^3)	N_{Br}	N_F	k (cm^3 molecule^{-1} s^{-1})	$k_{average}$ (cm^3 molecule^{-1} s^{-1})
CH_3Br	3.05	1	0	5.3×10^{-12} [5], 1.0×10^{-11} [8], 5.8×10^{-12} [9], 6.0×10^{-12} [11,25], 5.0×10^{-12} [33], 3.6×10^{-12} [7], 7×10^{-12} [6], 6.7×10^{-12} [10], 1.08×10^{-11} [12], 6.3×10^{-12} [28]	6.6×10^{-12}, 6.5×10^{-12} [26]
CF_3Br	4.73	1	3	1.6×10^{-8} [11], 1.5×10^{-8} [16,29], 8.6×10^{-9} [15], 1.36×10^{-8} [29,32], 1.2×10^{-8} [25,28]	1.3×10^{-8}, 1.4×10^{-8} [26]
CH_2Br_2	6.10	2	0	9.3×10^{-8} [11], 3.5×10^{-8} [25], 9.0×10^{-8} [17], 3.2×10^{-8} [32], 1.06×10^{-7} [18]	7.1×10^{-8}, 9.6×10^{-8} [26]
CF_2Br_2	7.22	2	2	1.7×10^{-7} [30], 2.6×10^{-7} [31,32], 3.0×10^{-7} [18,20,34,35]	2.7×10^{-7}, 2.6×10^{-7} [26]
$CHBr_3$	9.15	3	0	4.3×10^{-8} [30]	
$CFBr_3$	9.71	3	1	3.0×10^{-9} [30], 4.8×10^{-9} [20,34,35]	4.4×10^{-9}
CBr_4	12.20	4	0	2.5×10^{-8} [30]	
CH_3CH_2Br	3.05	1	0	5.3×10^{-12} [13], 2.8×10^{-13} [6], 9.0×10^{-11} [14]	5.0×10^{-12}, 1.4×10^{-10} [26]
CH_2FCH_2Br	3.33	1	0.5	5.0×10^{-11} [present data], 1.3×10^{-9} [19]	
CF_3CH_2Br	3.89	1	1.5	1.4×10^{-9} [present data], 1.5×10^{-8} [19]	
CH_2BrCH_2Br	4.57	1.5	0	1.8×10^{-8} [present data]	
CH_2BrCF_2Br	5.69	1.5	2	1.7×10^{-7} [19], 1.5×10^{-8} [20]	9.2×10^{-8}
CH_3CHBr_2	6.10	2	0	4.1×10^{-8} [19,26,27], 1.5×10^{-8} [20]	3.5×10^{-8}
CF_2BrCF_2Br	6.25	1.5	3	1.3×10^{-7} [19], 1.6×10^{-7} [20]	1.4×10^{-7}
CF_3CFBr_2	7.50	2	2.5	1.6×10^{-7} [20], 1.6×10^{-7} [34]	1.6×10^{-7}
$CH_2BrCHBr_2$	7.63	2.5	0	9.2×10^{-8} [19]	
$CHBr_2CHBr_2$	9.15	3	0	6.9×10^{-8} [18], 1.2×10^{-7} [19]	9.5×10^{-8}
$CH_3CHBrCH_3$	3.05	1	0	1.4×10^{-12} [present data]	
$CH_3CH_2CH_2Br$	3.05	1	0	1.1×10^{-11} [present data]	

electron affinity of the molecule or that of the electronegative atom.

As it was pointed out recently by Klar et al. [36], the long range electron non-polar molecule interaction is described by the polarization potential depending on the electronic polarizability $V(r) = -\alpha e^2/2r^4$. This leads to the threshold cross-section for s-wave capture at low energies, $\sigma(E \to 0)$, proposed by Vogt and Wannier [37]:

$$\sigma(E \to 0) = 4\pi a_0^2 \left(\frac{\alpha}{2E}\right)^{1/2} \quad (7)$$

where a_0 is the Bohr radius, α is the polarizability and E is an electron energy. Thus, the polarizability of the molecule is the essential factor deciding on the thermal electron capture rate constant.

Permanent dipole moment causes some additional interaction which should increase the electron capture cross section to some extent. Accordingly to their estimation this effect can be neglected at α around 9×10^{-24} cm^3 and μ around 0.5 D. This led them to the formula (8) for the thermal electron capture rate constant:

$$k_{\text{th}} = 4 \times 10^{-8} \alpha^{1/2} \text{ cm}^3 \text{ molecule}^{-1} \text{ s}^{-1} \quad (8)$$

where α values are expressed in 10^{-24} cm^3 units.

Using literature values for α (9.45×10^{-24} and 10.7×10^{-24} cm^3 for $CFCl_3$ and 1,1,1-$C_2Cl_3F_3$) they have obtained $k = 6.2 \times 10^{-7}$ and 6.6×10^{-7} cm^3 molecule^{-1} s^{-1}, respectively. These are essentially in good agreement with the experimental ones. However, Eq. (8) can be applied only to the highly halogenated alkanes, for which the thermal s-wave electron cross-section approaches its limiting value $\pi\lambda^2$, where λ is the reduced de Broglie wavelength. This corresponds to $k_{\text{th}} \approx 4 \times 10^{-7}$ cm^3 molecule^{-1} s^{-1}. For other compounds the dependence of the experimental thermal rate constants on their polarizability is also observed, but it is much stronger than that following from Eq. (8). In fact, it is rather exponential. The second observation is that k_{th} actually does not depend on the polarizability of the molecule as a whole but on the summary polarizability of the halogen atoms at the carbon atom where the capture occurs.

We have previously proposed [4,21–23] an empirical correlation between the rate constant for the electron capture and the polarizability of the attaching center, α_{center}. As an attaching center we consider that part of the molecule which is immediately connected with the attachment process, e.g., in the case of $C_nH_{2n-m+2}Hal_m$ α_{center} is a sum of polarizabilities of halogen atoms calculated using additivity rule, while carbon and hydrogen atoms should be eliminated from consideration. The preliminary analysis shows that in the case when halogens are placed at neighboring carbon atoms the best correlation is obtained if one calculates first the sum of polarizabilities at each carbon and then takes the higher value with coefficient 1 and the other one with coefficient 0.5 (see Table 1). The corresponding α_{center} values calculated using $\alpha_F = 0.557 \times 10^{-24}$ cm^3 and $\alpha_{Br} = 3.05 \times 10^{-24}$ cm^3 are included in Table 1.

An inspection of Table 1 shows that most of the k values for CH_3Br lie in the range (5–10) $\times 10^{-12}$ cm^3 molecule^{-1} s^{-1} and average value of 6×10^{-12} cm^3 molecule^{-1} s^{-1} can be safely proposed as the well established one, as it was also made by Christophorou [26]. The data for CH_3CH_2Br are scattered over three orders of magnitude, however, our value [13] lies also in this region as well as our present value for $CH_3CH_2CH_2Br$. There are no other experimental data for 1-bromoalkanes to analyze the influence of the chain length on the electron capture process. However, Aflatooni and coworkers [38–40] have measured vertical attachment energy (VAE) for a set of chloro- and chlorofluoroalkanes using electron transmission spectroscopy. In particular, they determined VAE for all 1-chloroalkanes up to 1-chlorooctane and found no influence of the chain length on this value. Thus, we can suppose that this applies also to the rate constants and take our values for CH_3CH_2Br and $CH_3CH_2CH_2Br$ as correct ones. This is compatible with our supposition that only the polarizability of halogen atoms influence the electron capture process and not that of a molecule as a whole.

Finally, Fig. 5 shows that potential curves for C–Br and C–Br$^-$ are practically the same for all three compounds. Thus, this also shows that carbon length does not change the capture process. At this point we can recommend the rate constant for all three compounds to be the same and equal to $(6 \pm 2) \times 10^{-12}$ cm^3 molecule^{-1} s^{-1}.

The rate constant for $CH_3CHBrCH_3$ is by an order of magnitude lower than that for 1-bromopropane in spite of that α is the same. As this is the first value for 2-substituted alkane one can suspect that it is caused by a different steric factor, but more data are needed to make a proper judgment.

The next observation is that adding additional bromine causes drastic increase in the rate constant by four orders of magnitude, almost to the limiting value. Further increase of α_{center} has much smaller effect. Thus, changes in this region can be observed only by changing the number of the fluorine atoms. Unfortunately, there are only a few data in this region and among them two, for CH_2FCH_2Br and CF_3CH_2Br, for whose Sunagawa and Shimamori [19] values are by an order of magnitude bigger than ours. Taking into account that fluorine atom causes rather small changes in the rate constant (cf. also ref. [26] for chlorofluoroalkanes), especially at neighboring carbon, we would rather suspect that their values are too big (probably because of some highly brominated impurities).

The plot of the rate constant versus α_{center} in log scale is shown in Fig. 3. The average data together with those from four different laboratories are shown. If one removes the data which should not be considered accordingly to above discussion (denoted as diamonds in Fig. 3), it can be clearly seen that the rate constant increases strongly, by 4 orders of magnitude, while α_{center} changes from 3×10^{-24} to ca. (6–7) $\times 10^{-24}$ cm^3. Further increase in α_{center} changes the k value to much lower extent. This can be rationalized in terms of potential energy curves for the neutral molecule and transient negative ion.

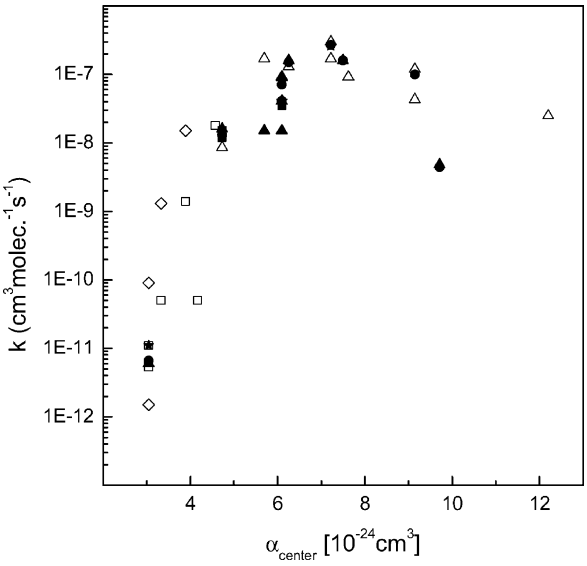

Fig. 3. The dependence of the electron capture rate constant on α_{center} for compounds from Table 1: (□), our data (present ones and those from refs. [5,13]); (★), Christophorou et al.; (△), Shimamori et al.; (▲), Smith et al.; (■), McFadden et al.; (●), averaged literature data (cf. Table 1), (◇), data to be removed (see text).

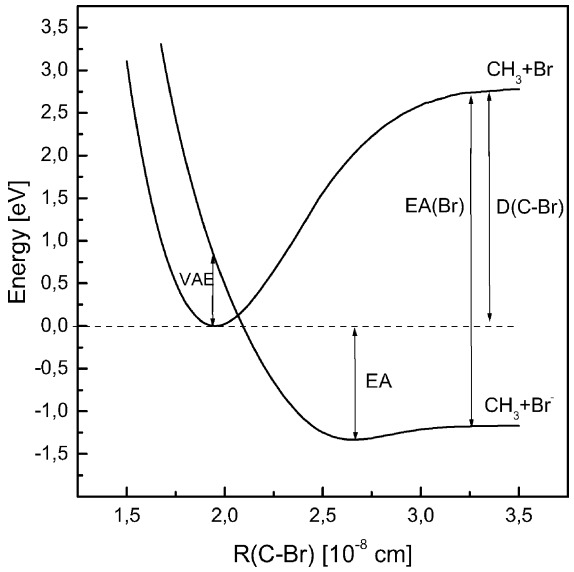

Fig. 4. The Morse curves for methyl bromide and its negative ion.

The dependence of a capture cross-section on energy has a resonant form, which is a result of a Franck–Condon transition from the ground vibrational level of the neutral to the transient negative ion. For electrons with thermal energy distribution as in all cases presented in Table 1, this transition can be probable if curve crossing occurs nearby the lowest vibrational level of the neutral.

If however the resonance lies high above thermal region then the probability of such a transition at thermal electron energy distribution is rather low and another mechanism should be involved. It is based on the fact that even at room temperature the higher vibrational levels are partly populated. The F–C transition from these levels requires much less electron energy, available at thermal distribution. In this case the rate constant or, in fact, activation energy depends on the level of the crossing of the potential energy curves for the neutral and transient negative ion.

To rationalize this statement we have performed calculations of the structure of the molecules and corresponding molecular negative ions using a semi-empirical SCF PM3 method. We have analyzed the influence of bromine and fluorine atoms placed in different number at different carbon atoms of halomethanes, ethanes and propanes. This method allows calculating the energetically optimized structure (angles, bond lengths and total or/and binding electronic energy) both of the molecule and its negative ion. Applying potential function one can also build a whole potential energy curve for a particular bond with residual structure frozen. The example set of curves for methyl bromide is shown in Fig. 4.

The validity of the calculations can be estimated by comparison of the obtained parameters with available experimental values: the equilibrium C–Br bond length, R_{eq}(C–Br) = 1.95 (calc.) and 1.933 cm^{-8} (exp.), the C–Br bond energy, D(C–Br) = 2.8 (calc.) and 3.04 ± 0.05 eV (exp.), the bromine atom electron affinity, EA(Br) = 3.9 (calc.) and 3.37 eV (exp.) as well as the H–C–H angle, ∠HCH = 110.5 (calc.) and 111.2° (exp.). The experimental data were taken from ref. [24]. The calculated values are not far from the experimental ones and it seems that they can be used safely for comparison purposes.

As can be seen, the curve for negative ion is shifted toward the longer equilibrium internuclear distances. For big enough bond elongation the potential curve crossing occurs on the right side of the curve for neutral. The energy of the F–C transition is too high to be reached by electrons at a thermal energy distribution. Thus, in this case we expect the electron capture to occur at much lower energy of the curve crossing where both electron energy and that of higher vibrational states of the molecule add to probability of the reaction.

Fig. 5 shows that the carbon chain length has minor influence on the position and form of the neutral and ion potential curves when going from methyl to 1-propyl bromide and one would not expect strong change in the rate constant for these compounds. Inspection of Table 1 shows that our data for methyl, ethyl and 1-propyl bromide (5.3, 5.3 and 11×10^{-12} cm^3 $molecule^{-1}$ s^{-1}, respectively) together with well established average value for methyl bromide agree well with this statement.

Fig. 6 shows the potential curves for C–Br bond in CH_3CH_2Br, CH_2BrCH_2Br, CH_3CHBr_2 and CH_3CBr_3. It is seen that adding bromine atom in position one decreases only slightly the calculated C–Br bond length and its strength, in agreement with experimental data. In the same time the potential curves for the negative ions are shifted to the right. The shift decreases with the number of the

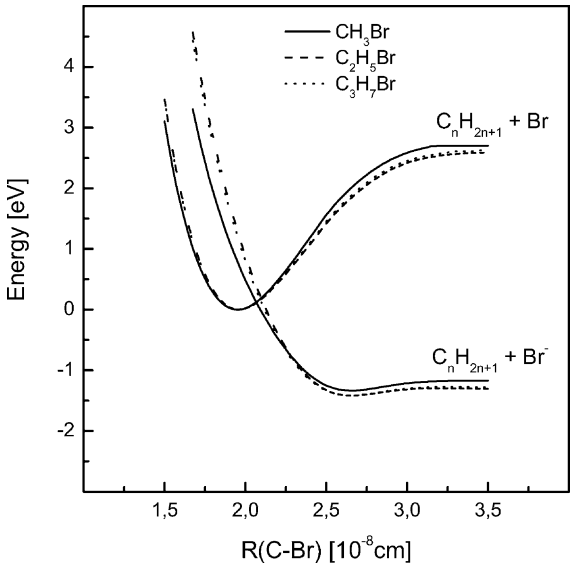

Fig. 5. Morse curves for the neutral molecules CH_3Br, C_2H_5Br and C_3H_7Br and their negative ions.

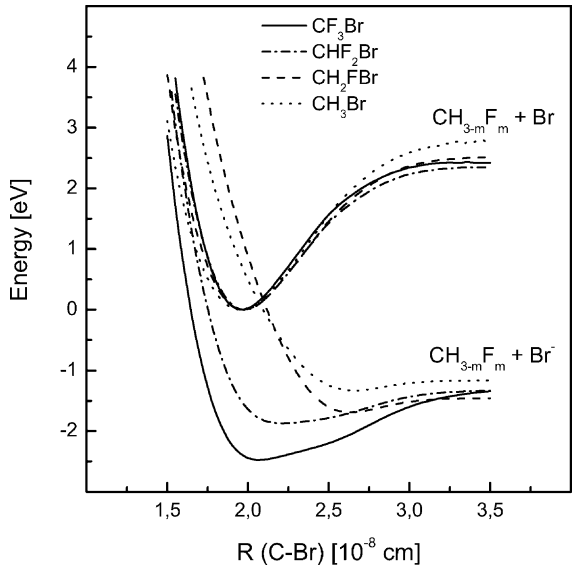

Fig. 7. Morse curves for bromofluoromethanes and their negative ions.

Br atoms. Simultaneously we observe increase in adiabatic electron affinity. In effect, while the curves for ethyl bromide cross above the minimum for neutral, the ones for other ions "envelope" the neutral curve. This leads to quite significant activation energy and relatively low rate constant for thermal electron capture by ethyl bromide and zero activation energy and high rate constant for the others. In the case of CH_2BrCH_2Br the calculated negative ion curve lies much lower than expected in series and we cannot explain this behavior.

Fig. 7 demonstrates the influence of a consecutive replacement of hydrogen atoms by fluorine in methyl bromide. Also in this case we observe shortening the negative ion bond length and increase in electron affinity with the number of the fluorine atoms in the molecule.

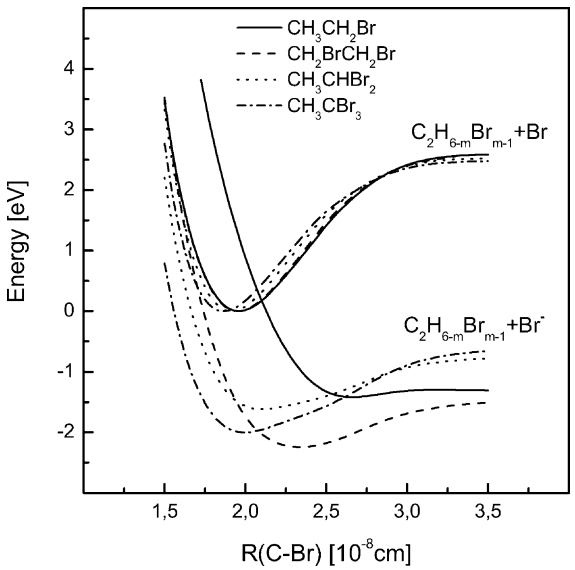

Fig. 6. Morse curves for bromine substituted ethanes and their negative ions.

Summarizing, let us now return to Fig. 3. It can be seen that the dependence of the rate constant for thermal electron capture on the polarizability both for fluorinated and non-fluorinated bromides reflects mainly the shortening of the C–Br bond length in the negative ion connected with distribution of the additional charge among the bromine atoms. The last actually means formation of a new, joint orbital occupied by the incoming electron. This leads to shifting the curve crossing to lower energies (decreasing the activation energy) at α_{center} below ca. $(4–5) \times 10^{-24}\,cm^3$ and enveloping the curves above this value. The last should mean zero activation energy. Apparent increase in k values for fluorinated compounds over those for non-fluorinated can be ascribed to the fact that the electron affinity does not depend on α_{center} but rather on the number of halogen atoms. All together seems to indicate that the change in the dependence of the rate constant on the polarizability at $\alpha_{center} \approx (6–7) \times 10^{-24}\,cm^3$ is caused by diminishing activation energy to zero above this value.

Much more experimental data on the rate constants as well as beam data for energy dependence of electron capture cross-section are required to go into detail analysis, also to confirm reliability of the calculated features. In the parallel paper [41] we present similar results for chlorine-containing alkanes, which are well compatible with the present ones.

Acknowledgements

The research was supported by KBN under grant 3 T09A 010 18.

References

[1] I. Szamrej, W. Tchórzewska, H. Kość, M. Foryś, Radiat. Phys. Chem. 47 (1996) 269.
[2] I. Szamrej, J. Jówko, M. Foryś, Radiat. Phys. Chem. 48 (1996) 65.
[3] I. Szamrej, H. Kość, M. Foryś, Radiat. Phys. Chem. 48 (1996) 69.
[4] A. Rosa, W. Barszczewska, M. Foryś, I. Szamrej, Int. J. Mass Spectrom. 205 (2001) 85.
[5] I. Szamrej, H. Kość, M. Foryś, B.M. Zhytomirsky, B.G. Dzantiev, Radiat. Phys. Chem. 38 (1991) 541.
[6] K.M. Bansal, R.W. Fessenden, Chem. Phys. Lett. 15 (1972) 21.
[7] K.G. Mothes, E. Schultes, R.N. Schindler, J. Phys. Chem. 76 (1972) 3758.
[8] G.R.A. Johnson, M.C. Sauer, J.M.J. Warman, Chem. Phys. 50 (1969) 4933.
[9] W.C. Wang, L.C. Lee, J. Appl. Phys. 63 (1988) 4905.
[10] Z.Lj. Petrović, R.W. Crompton, J. Phys. B 20 (1987) 5557.
[11] E. Alge, N.G. Adams, D. Smith, J. Phys. B. 17 (1984) 3827.
[12] P.G. Datskos, L.G. Christophorou, J.G. Carter, J. Chem. Phys. 97 (1992) 9031.
[13] W. Barszczewska, A. Rosa, J. Kopyra, I. Szamrej, Res. Chem. Intermed. 27 (2001) 699.
[14] A.A. Christodoulides, L.G. Christophorou, J. Chem. Phys. 54 (1971) 4691.
[15] H. Shimamori, Y. Tatsumi, Y. Ogawa, T. Sunagawa, J. Chem. Phys. 97 (1992) 6335.
[16] J.M. Christopher, T. Cheng-ping, L.M. David, J. Chem. Phys. 19 (1989) 2194.
[17] H. Shimamori, Y. Tatsumi, Y. Ogawa, T. Sunagawa, Chem. Phys. Lett. 194 (1992) 223.
[18] S.H. Alajajian, M.T. Bernius, A. Chutjian, J. Phys. B 21 (1988) 4021.
[19] T. Sunagawa, H. Shimamori, Int. J. Mass Spectrom. Ion Proc. 149 (1995) 123.
[20] D. Smith, C.R. Herd, N.G. Adams, J.F. Paulson, Int. J. Mass Spectrom. Ion Proc. 96 (1990) 341.
[21] I. Szamrej, Gaseous Dielectrics, vol. VIII, Kluwer Academic/Plenum Publishers, New York, 1998, p. 63.
[22] M. Foryś, I. Szamrej, J. Radioanal. Nucl. Chem. 232 (1998) 67.
[23] A. Rosa, M. Foryś, I. Szamrej, Gaseous Dielectrics, vol. VIII, Kluwer Academic/Plenum Publishers, New York, 1998, p. 69.
[24] CRC Handbook of Chemistry and Physics, 73rd ed., CRC Press, Boca Raton, FL, 1992–1993.
[25] S.J. Burns, J.M. Matthews, D.L. McFadden, J. Phys. Chem. 100 (1996) 19436.
[26] L.G. Christophorou, Z. Phys. Chem. 195 (1996) 195.
[27] H. Shimamori, Y. Nakatani, Chem. Phys. Lett. 150 (1988) 109.
[28] R.G. Levy, S.J. Burns, D.L. McFadden, Chem. Phys. Lett. 231 (1994) 132.
[29] C.J. Marotta, C. Tsai, D.L. McFadden, J. Chem. Phys. 91 (1989) 2194.
[30] T. Sunagawa, H. Shimamori, J. Chem. Phys. 107 (1997) 7876.
[31] T.G.J. Lee, Phys. Chem. 67 (1963) 360.
[32] R.P. Blaunstein, L.G. Christophorou, J. Phys. Chem. 49 (1968) 1526.
[33] W.E. Wentworth, R. George, H.J. Keith, Chem. Phys. 51 (1969) 1971.
[34] D. Smith, P. Spanel, Adv. Atom. Mol. Opt. Phys. 32 (1994) 307.
[35] R.W. Crompton, G.N. Haddad, R. Hegerberg, A.G. Robertson, J. Phys. B 15 (1982) L483.
[36] D. Klar, M.-W. Ruf, I. Fabrikant, H. Hotop, J. Phys. B 34 (2001) 3855.
[37] E. Vogt, G.H. Wannier, Phys. Rev. 95 (1954) 1190.
[38] K. Aflatooni, P.D. Burrow, Int. J. Mass Spectrom. 205 (2001) 149.
[39] K. Aflatooni, P.D. Burrow, J. Chem. Phys. 113 (2000) 1455.
[40] K. Aflatooni, G.A. Gallup, P.D. Burrow, Chem. Phys. Lett. 282 (1998) 398.
[41] W. Barszczewska, J. Kopyra, J. Wnorowska, I. Szamrej, J. Phys. Chem. A 107 (2003) 11427.